Simulation of flows in shock-tube facilities by means of a detailed chemical mechanism for nitrogen excitation and dissociation

By A. Bourdon†, M. Panesi‡, A. Brandis¶, T. E. Magin, G. Chaban, W. Huo, R. Jaffe AND D. W. Schwenke

A database was recently developed at NASA Ames Research Center for the dissociation and excitation rates of the rovibrational energy levels of nitrogen. This work is a first step toward the development of a simplified mechanism for 3-D simulations of atmospheric entry flows. First, we have derived a Boltzmann average dissociation rate based on rotational and vibrational temperatures. At thermal equilibrium, a very good agreement is obtained with the rate proposed by Park (1990). Significant discrepancies are observed in thermal non-equilibrium conditions. Then, we have developed a 0-D vibrational state-to-state collisional model to simulate a typical shock in a nitrogen flow based on vibrational-specific excitation and dissociation reaction rates derived by assuming a Boltzmann distribution of the rotational energy levels at the translational temperature. We have shown that the vibrational energy relaxation for the monoquantum excitation processes deviates significantly from the conventional Landau-Teller law. The dissociation process, coupled with the energy level relaxation dynamics, strongly depends on multi-quantum jump processes. Finally, we have implemented the multi-temperature dissociation rate in a 1-D code for shock-tube flows and have compared our results with experimental results.

1. Introduction

Prediction of the convective and radiative heat fluxes to the surface of a spacecraft entering a planetary atmosphere strongly depends on the completeness and accuracy of the physical model used to describe the non-equilibrium phenomena into the flow. During an atmospheric entry, the translational energy of the fluid particles drastically rises through a shock. Depending on the intensity of the shock, different physico-chemical processes may take place, such as excitation of the internal energy modes, dissociation of the molecules, ionization of the atoms and molecules. These non-equilibrium phenomena are strongly coupled to each other. For re-entry velocities >10 km/s, a significant portion of the heating experienced by the heat shield can be due to radiation and is highly influenced by the shape of the internal energy distribution function. Concentration of the gas species and distribution of their internal energy level populations can be estimated by means of either multi-temperature models (Park 1990) or collisional radiative (CR) models (Laux 2002; Bultel *et al*. 2006).

In multi-temperature models, the physico-chemical properties of the air flow are obtained by assuming that, for all the species, the population of each internal energy mode

† EM2C, CNRS – Ecole Centrale Paris, France
‡ von Karman Institute for Fluid Dynamics, Belgium
¶ University of Queensland, Australia

follows a Boltzmann distribution at its own temperature (T_r rotational, T_v vibrational, or T_e electronic temperature, respectively). These models have been developed based on experimental data obtained in flight and also in high-enthalpy facilities representative of specific flight conditions, such as in arc-jet and shock-tube windtunnels (Park 1990). The problem with this approach is that the models can contain many uncertainties that can be extremely difficult to quantify. Moreover, there is no detailed information about the specific state of the gas since these data are highly averaged (e.g., stagnation point heat-flux measurement). Park (1990) and (2006) has worked extensively on multi-temperature models for air and has also shown that the use of these models, even if very efficient from a computational point of view, can only be justified when the departure from the Boltzmann population is small, i.e., for low-velocity and high-pressure re-entry conditions.

Collisional radiative models take into account all relevant collisional and radiative mechanisms between the internal energy levels of the different species in the flow. They constitute a valid alternative to the multi-temperature models since they exhibit a larger spectrum of applicability. By increasing order of complexity and computational time, three kinds of CR models can be distinguished for air: *electronic*, *vibrational* and *rovibrational* CR models. In electronic CR models, transitions between the electronic states are considered and the rovibrational levels of the molecules are populated according to Boltzmann distributions at temperatures T_r and T_v. In vibrational CR models, transitions between the vibrational states of the molecules are also considered and only a rotational temperature T_r is defined. Finally, in rovibrational CR models, no temperature is required to describe the internal energy. The quality of the results obtained with a CR model mainly relies on the accuracy of the rate coefficients for elementary processes between energy levels. Different theoretical models have been developed in the literature to determine elementary rate coefficients: for instance, the quasiclassical trajectory method using a potential energy surface which is a fit to *ab initio* electronic structure calculations (Schwenke 1990), the same method based on approximate energy surfaces (Esposito *et al.* 2006) and the analytical theory of the forced harmonic oscillator (Macheret *et al.* 2000). Recently, the computational chemists at NASA Ames Research Center have embarked on the characterization of non-equilibrium air chemistry from first principles (Jaffe *et al.* 2008; Schwenke *et al.* 2008). So far, the N, N_2 system has been studied to yield rate coefficients and cross-sections for molecular excitation and dissociation of the rovibrational energy levels of molecular nitrogen in the ground electronic state. First principle calculations are used to generate realistic nuclear interaction potentials. Then, the quasiclassical trajectory method yields the fundamental data required for a rigorous treatment of non-equilibrium chemistry.

The present work is at the interface between computational chemistry and computational fluid dynamics by developing new models based on microscopic theory and applying them to macroscopic scale. We propose to use the database recently developed at NASA Ames Research Center to derive multi-temperature dissociation rates for molecular nitrogen and compare them with literature results. Then, we will develop a 0-D vibrational state-to-state collisional model to simulate a typical shock in a nitrogen flow. We will also assess the validity of the conventional Landau-Teller relaxation model for vibrational excitation based on a harmonic oscillator and monoquantum jumps. Finally, we will implement the multi-temperature dissociation rate derived in this work into a 1-D shock-tube code and compare our results with experimental measurements.

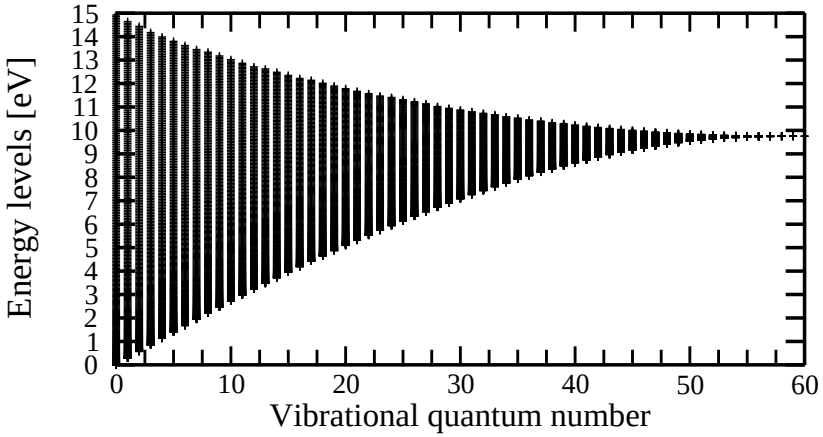

FIGURE 1. Rovibrational energy levels of molecular nitrogen in the electronic ground-state as a function of the vibrational quantum number v. Each cross corresponds to a (v, J) rovibrational level. The dissociation energy of N_2 in the electronic ground-state is 9.75 eV.

2. Energy levels and detailed excitation and dissociation chemical mechanism

The NASA Ames database comprises 9390 (v, J) rovibrational levels for the electronic ground-state of nitrogen. These levels can also be denoted by means of a global index i, sorting them as a function of their vibrational quantum number v and then considering their rotational quantum number J. The relation between both i and (v, J) notations is expressed as

$$E(i) = E_v + \Delta E_{v,J}, \quad i = 1, \ldots, i_{max}, \tag{2.1}$$

where the vibrational contribution reads $E_v = E(v, 0)$, and the rotational contribution $\Delta E_{v,J} = E(v, J) - E(v, 0)$, $v = 0, \ldots, v_{max}$, $J = 0, \ldots, J_{max}(v)$. This approach, widely used for simplified models for the distribution of rovibrational levels (e.g., Morse oscillator and rigid rotator), is selected here to easily compare our results with the literature. However, Fig. 1 shows that separation of the rotational and vibrational energy modes is rather arbitrary at energies higher than 1 eV typical of atmospheric entry applications. Other sorting methods to determine index i are also possible, for example, a complementary approach is sorting the energy levels as a function of their rotational quantum number J and then considering their vibrational quantum number v, with the same energy mode separation drawback. Finally, an alternative approach that we are currently studying is lumping the levels as a function of their global internal energy, independently of their vibrational and rotational contributions.

Fig. 1 shows that most of the energy levels are truly bound (i.e., their energy is lower than the dissociation energy E_{vmax}=9.75 eV of the electronic ground-state of nitrogen), while some of them are quasibound (i.e., their energy is higher than the dissociation energy). The NASA Ames database comprises more than 23 million reaction rates for dissociation of truly bound states and quasibound states and excitation between all states for six values of the gas translational temperature (7500; 10,000; 12,500; 15,000; 20,000 and 25,000 K). It is important to mention that not only monoquantum but also multiquantum processes are accounted for (Jaffe *et al.* 2008; Schwenke *et al.* 2008). We have used all endothermic rates to derive reverse rates based on microreversibility although some exothermic rates were also available. For a given elementary process, the value of the exothermic rate is always higher than the endothermic one, then, the accuracy of the

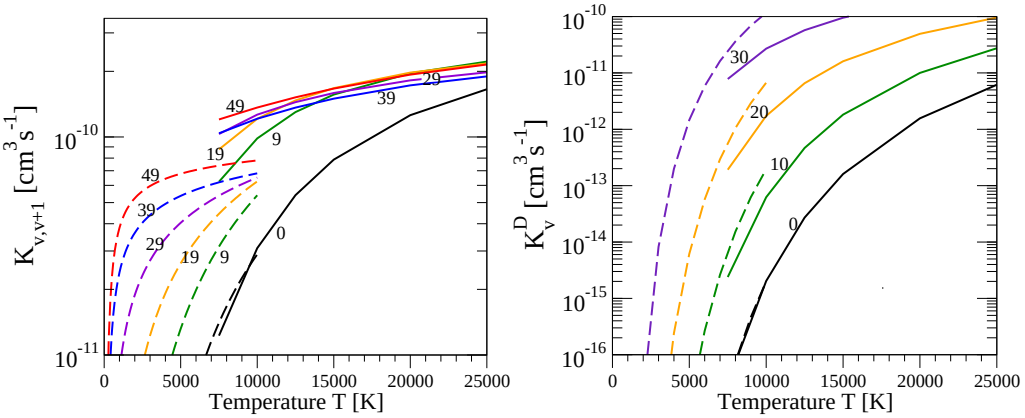

FIGURE 2. Vibrational-specific rates as a function of the temperature T obtained by assuming a Boltzmann distribution of the rotational energy levels at the temperature $T_r = T$. Left: monoquantum excitation process $N_2(v) + N \rightarrow N_2(v+1) + N$, for $v = 0, 9, 19, 29, 39, 49$; right: dissociation process $N_2(v) + N \rightarrow 3N$, for $v = 0, 10, 20, 30$. NASA Ames database (unbroken lines); Esposito *et al.* (2006) (dashed lines).

calculated exothermic rates is better than the one of endothermic rates. It would be interesting to study the influence on the results of using exothermic rates (when available) to derive reverse rates.

Fig. 2 shows the vibrational specific rate for the monoquantum excitation process $N_2(v) + N \rightarrow N_2(v+1) + N$ and dissociation process $N_2(v) + N \rightarrow 3N$ for different values of v as a function of the temperature T assuming a Boltzmann distribution for the rotational energy levels at temperature $T_r = T$. The rates, calculated by using the the NASA Ames database, are compared with the rates calculated up to 10,000 K by Esposito *et al.* (2006). Over the limited temperature range $(7500 - 10,000\,\mathrm{K})$ where both databases overlap, we note a very good agreement for the level $v = 0$ and a significant discrepancy for higher values of v. However, the relative temperature evolution of the rates for $v = 9$ up to 49 is very similar for both databases. It is important to mention that, as the high-lying energy levels of both databases are different, it would be more relevant to compare the rates for levels with the same energy value and not for levels with the same vibrational quantum number.

3. Multi-temperature dissociation rates

To compare our results with the multi-temperature dissociation rates available in the literature, we have averaged the microscopic dissociation rates $K^D_{vJ}(T)$ for the (v,J) rovibrational levels over Boltzmann distributions at the rotational (T_r) and vibrational (T_v) temperatures for the internal energy. The resulting multi-temperature dissociation rate is given by the expression

$$K^D(T, T_r, T_v) = \frac{1}{Q_{int}(T_r, T_v)} \sum_{v=0}^{v_{max}} \exp\left(\frac{-E_v}{kT_v}\right) \sum_{J=0}^{J_{max}(v)} (2J+1) \exp\left(\frac{-\Delta E_{v,J}}{kT_r}\right) K^D_{vJ}(T), \quad (3.1)$$

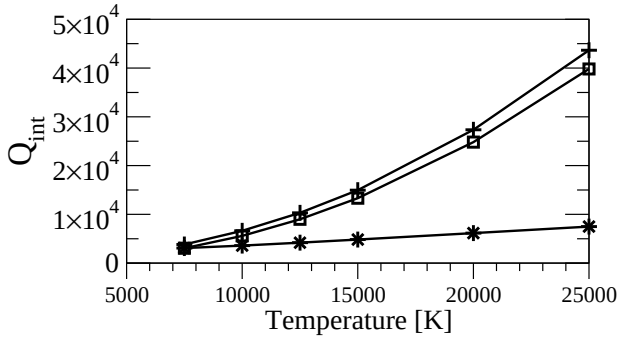

FIGURE 3. Partition function $Q_{int}(T_r, T_v)$ at thermal equilibrium ($T_r = T_v$). NASA Ames database (line with crosses); Park (1990) (line with squares); harmonic oscillator approximation (line with stars).

where the internal energy partition function $Q_{int}(T_r, T_v)$ reads

$$Q_{int}(T_r, T_v) = \sum_{v=0}^{v_{max}} \exp\left(\frac{-E_v}{kT_v}\right) \sum_{J=0}^{J_{max}(v)} (2J+1) \exp\left(\frac{-\Delta E_{v,J}}{kT_r}\right). \tag{3.2}$$

The accuracy of the partition function depends on the quality of the potential surfaces used to calculate the energy levels, whereas the rates depend on both potential surfaces and quasiclassical trajectory calculations.

Fig. 3 compares the partition function calculated by means of Eq. (3.2) at thermal equilibrium ($T = T_r = T_v$) based on the energy levels of the NASA Ames database with the partition function based on energy levels obtained by assuming the harmonic oscillator and rigid rotor approximation. As expected, this simplified model is only valid at low temperatures for which only the low energy levels are significantly populated. At temperature $T = 20,000$ K, the partition function is under-estimated by a factor of 4. We have found a fair agreement with the results of Park (1990), the discrepancy between both models increasing with temperature.

Fig. 4 compares the dissociation rate given in Eq. (3.1) computed by means of the NASA Ames database with some widely used rates found in the literature for the temperature range $7500 - 25,000$ K. At thermal equilibrium ($T = T_r = T_v$), our computed dissociation rate agrees very well at the threshold temperature $T = 20,000$ K with the rate derived from shock-tube experiments by Park (1993). Our calculation, based on first principles data, predicts a lower value than the one obtained by Park for $T < 20,000$ K and a higher value for $T > 20,000$ K, the discrepancy between both rates increasing as temperature deviates from the threshold temperature. The rates proposed by Shatalov (1987) and Esposito *et al.* (2006) are very close to each other but over-estimate the dissociation rate by one order of magnitude. In thermal non-equilibrium conditions ($T = T_r \neq T_v$), we have found significant discrepancies between the dissociation rate derived from the NASA Ames database and the two-temperature rate proposed by Park (1993). For example, this rate is two orders of magnitude lower than our rate computed in thermal non-equilibrium at $T = T_r = 20,000$ K, $T_v = 3000$ K. We have also used the thermal equilibrium dissociation rate calculated by means of the NASA Ames database with the thermal non-equilibrium model proposed by Chernyi *et al.* (2004). It is inter-

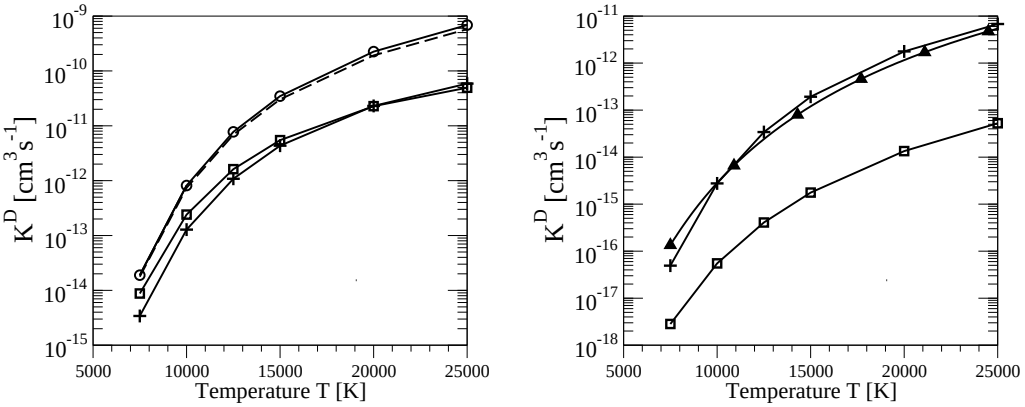

FIGURE 4. Boltzmann average dissociation rate $K^D(T, T_r, T_v)$. Left: thermal equilibrium ($T = T_r = T_v$); right: vibrational thermal non equilibrium ($T_r = T$, T_v=3000 K). NASA Ames database (lines with crosses); Park (1993) (lines with squares); Esposito *et al.* (2006) (dashed line); Shatalov (1987) (line with circles); Chernyi *et al.* (2004) (line with triangles).

esting to mention that the resulting rate is very close to the one derived in thermal non-equilibrium from the NASA Ames database.

4. Vibrational state-to-state collisional model

A 0-D vibrational state-to-state collisional model is developed here as a first step toward a more accurate description of the energy relaxation and dissociation processes in a nitrogen flow. We take into account the 61 vibrational energy levels of N_2 of the NASA Ames database, as well as all the averaged elementary rates for excitation and dissociation, assuming that, for each vibrational level, the rotational energy level populations follow a Boltzmann distribution at the translational temperature T. The N_2, N mixture is considered to be initially in local thermodynamic equilibrium at p=10,000 Pa pressure and T=4000 K translational temperature (i.e., there is 1% mole fraction of N). At $t = 0$ s, the translational temperature T is suddenly increased to a value of 20, 000 K, allowing for the temporal relaxation of the vibrational energy level populations to be studied (see Bultel *et al.* 2006, for the numerical method). The total vibrational energy reads

$$E_{vib}(t) = \sum_{v=0}^{v_{max}} n_v(t) E_v, \tag{4.1}$$

where n_v is the number density of the vibrational level v. We analyze the following cases:

(a) Monoquantum relaxation of the vibrational energy,

(b) Multi-quantum vibrational energy relaxation and multi-quantum dissociation,

in order to assess the validity of the Landau-Teller law and of the T, T_v dissociation rate derived in Sec. 3, respectively.

First, we study the vibrational energy relaxation by considering only monoquantum excitation/de-excitation processes $N_2(v)+N = N_2(v\pm1)+N$ and using the NASA Ames rates. Then, assuming that the vibrational energy relaxation is governed by a harmonic oscillator and that the excitation rate is given by the expression $K_{v+1,v} = (v + 1)K_{1,0}$, we obtain the Landau-Teller law

$$\frac{dE_{vib}}{dt} = \frac{-(E_{vib} - E^{\star}_{vib})}{\tau},$$

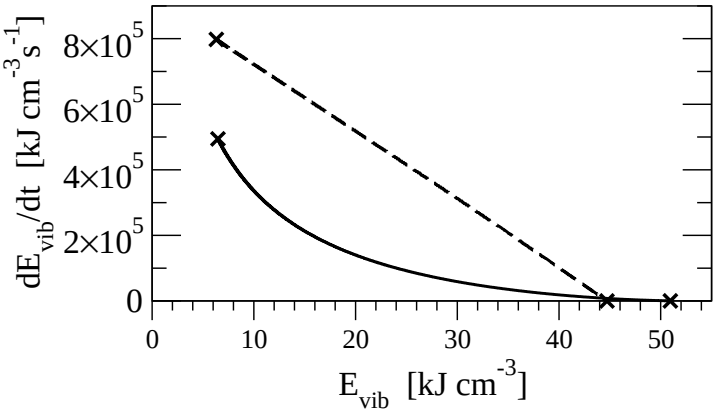

FIGURE 5. Trajectory in the phase space $(dE_{vib}/dt, E_{vib})$ for a N_2, N mixture starting from a local thermodynamic equilibrium state (p=10,000 Pa, T=4000 K, N mole fraction =1%). Monoquantum excitation processes are induced at t=0 s by a sudden change in temperature from T = 4000 to 20,000 K. NASA Ames database (unbroken line), Landau-Teller model (dashed line).

where quantity τ is a relaxation time and $E^{\star}_{vib}$ the total vibrational energy based on a vibrational energy level population following a Boltzmann distribution at the translational temperature T. This law is often used for the multi-temperature models implemented in computational fluid dynamic codes. Fig. 5 shows that the trajectory in the phase space $(dE_{vib}/dt, E_{vib})$ obtained by using the NASA Ames rates deviates from the straight line corresponding to the Landau-Teller law based on the rotationally averaged rate $K_{1,0}$ of the NASA Ames database. The relaxation time for vibrational energy depends on the vibrational energy distribution: the vibrational energy relaxation is very fast on short time scales and slows down as the vibrational distribution comes close to equilibrium. The total vibrational energy obtained at equilibrium depends on the vibrational energy levels. For the Landau-Teller model, we have used the 33 vibrational energy levels obtained by means of a harmonic oscillator based on the first quantum jump $E_1 - E_0$. This first result shows that the NASA Ames database allows for more accurate vibrational relaxation models to be derived for computational fluid dynamic applications.

Second, we study dissociation of molecular nitrogen by considering all elementary processes (multi-quantum excitation and dissociation). Fig. 6 shows the temporal evolution of the number densities of N and N_2. As expected, we note that molecular nitrogen rapidly dissociates: for $t > 10^{-5}s$, the system reaches the new thermodynamic equilibrium state at p=10,000 Pa and T= 20,000 K. Fig. 7 shows the vibrational distribution of N_2 at different times. We note that the populations of all vibrational levels evolve very rapidly, emphasizing the significant influence of multi-quantum excitation/de-excitation processes. Finally, Fig. 6 also shows the temporal evolution of the N number density calculated with different models: first the vibrational state-to-state collisional model, then the multi-temperature dissociation rate derived in Sec. 3 at thermal equilibrium and finally the rate of Park (1993) at thermal equilibrium. We note that in this simple testcase, the dissociation process is not accurately described by an effective multi-temperature rate

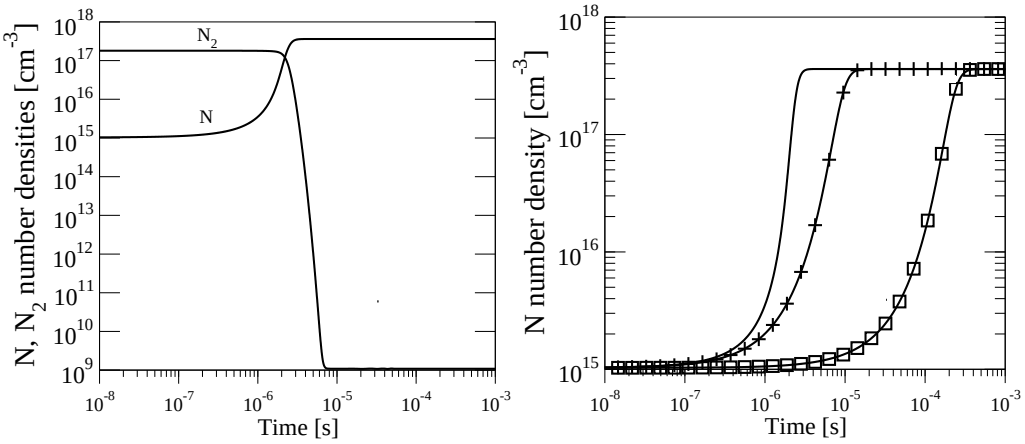

FIGURE 6. Temporal evolution of the number densities for a N_2, N mixture starting from a local thermodynamic equilibrium state (p=10,000 Pa, T=4000 K, N mole fraction =1%). Multi-quantum excitation and dissociation processes are induced at t=0 s by a sudden change in temperature from T = 4000 to 20,000 K. Vibrational state-to-state collisional model (unbroken lines), multi-temperature model based on the NASA Ames rate (line with crosses), multi-temperature model based on the Park (1993) rate (line with squares).

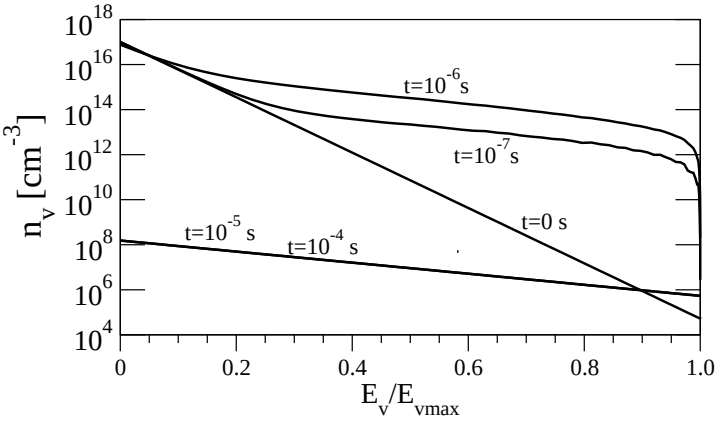

FIGURE 7. Vibrational energy distribution n_v for nitrogen obtained by means of the vibrational state-to-state collisional model at $t = 0,\ 10^{-7}, 10^{-6}, 10^{-5}, 10^{-4}$ s for the dissociation case given in Figure 6.

since the dissociation process is faster than the two multi-temperature dissociation rates at thermal equilibrium.

5. Validation with comparison with experiments

To assess the validity of the detailed chemical mechanism presented in this paper, comparisons were made with shock-tube data and other chemical models. The shock-tube data used for comparison was from the NASA Ames Research Center (Bose *et al.* 2005) and the University of Queensland (Brandis *et al.* 2008), where the radiation behind a strong shock was analyzed. The experiments presented were predominately aimed

at measuring the non-equilibrium radiation emitted from cyanogen in simulated Titan atmospheres. To compare with other models, several chemical mechanisms were implemented into a collisional radiative model.

The shock-tube experiments at the University of Queensland were conducted on the X2 shock-tube at various static pressures, shock speeds and chemical composition. This leads to a thorough data set for Titan entry, as well as a useful source for validation of CFD models. For the experiments presented in this paper, the facility was configured as follows. The driver was a mixture of helium and argon, the relative amounts of each depending on the condition, at a pressure of 300 mbar. The Titan gas used in these experiments was generally made up of 98% N_2 and 2% CH_4 giving the closest match to the lunar atmosphere. Additionally, tests were performed with other CH_4 concentrations to investigate its effect on the radiation intensity. In total, 270 shock-tube experiments were performed across approximately 30 conditions. The primary diaphragm separating the two gas mixtures was pre-scored 1.2 mm steel. The spectrometer mirror arrangement was set up so it resulted in a magnification of approximately 9 times. The amount of flow captured in each spectrograph exposure was 80 mm in length. The shock leaves the expansion tube as a planar wave. As the flow expands into the dump tank, the shock wave is bent by the expansion wave. By comparison, the EAST facility observes the radiating flow through windows in the shock-tube with the radiation traversing the boundary layer on the wall. At this stage, the difference between the flowfields has not been precisely quantified. The test times for these shots was approximately 60 microseconds, although this can change depending on the condition. This can be seen from the Pitot traces obtained just downstream of the region captured in the spectroscopy. Furthermore, this can also be matched up with the luminosity data obtained for the high-speed camera set up to capture each shot. The shock can be seen clearly on the camera footage, with a region of test gas following for a period of about 60 microseconds (corresponding to the steady region on the Pitot traces). When the driver gas interface arrives, the radiation is seen to stop. Fig. 8 shows a comparison between the NASA Ames EAST data and the data from the University of Queensland on the X2 facility. X2 and EAST have very similar wavelength profiles, however X2 shows approximately twice the amount of emitted radiance compared to EAST. As already mentioned, the fall-off rate is of particular importance for the validation of the computational chemistry models. It can be seen that if the power density is scaled so the that peaks match, the fall-off rate from both facilities matches extremely well.

To validate the models with the experiments, the different chemical mechanisms were implemented in a CR model. An electronic CR model was developed by Magin *et al.* (2004) to predict the non-equilibrium populations and the radiation of the excited electronic states CN(A,B) and N_2(A,B,C). The kinetic mechanism comprises spontaneous emission of the excited states, excitation/de-excitation by nitrogen and electron-impact collisions, pooling of N_2(A) and quenching of N_2(A) by excitation of CN(X) to CN(B). From the simulations run, it appeared that there was a significant discrepancy relating to the fall-off rate of the simulations. It was suggested that the reasons for the discrepancies were related to the reaction rates used in the simulation. From parametric variation of the reaction rates from the 19 species Titan model (Gökcen 2004), it was found that the molecular dissociation of nitrogen was the most influential reaction rate. Due to the importance of the N_2 concentration, it was decided to incorporate a vibrationally specific model to simulate the reaction of all the ground-state vibrational levels of N_2, known as the ViSpeN (Vibrationally Specific Nitrogen) CR model. The N_2 vibrationally

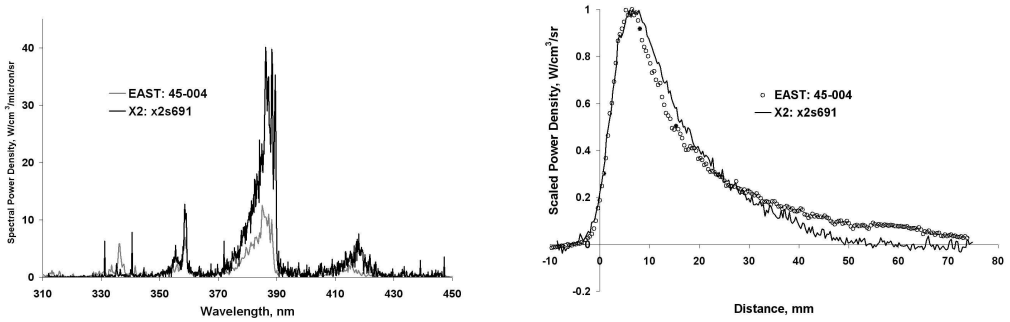

FIGURE 8. Experimental results obtained by means of the X2 (University of Queensland) and EAST (NASA Ames Research Center) facilities for 5.7 km/s velocity, 13 Pa pressure, $98\%N_2$ and $2\%CH_4$. Left: peak spectral power density; right: scaled power density integrated over $310 - 450$nm.

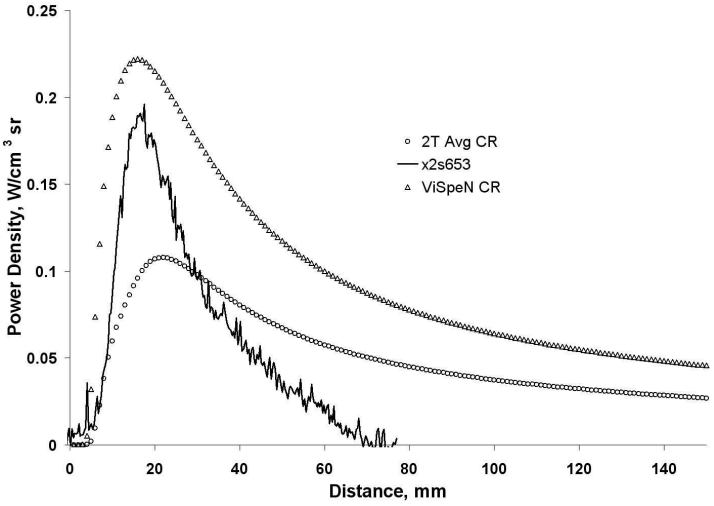

FIGURE 9. Comparison of computational models and X2 experiment (unbroken line) for 5.15 km/s velocity , 13 Pa pressure, $98\%N_2$ and $2\%CH_4$. Vibrational CR model ViSpeN (triangles), multi-temperature CR model (circles).

specific model used was developed by Pierrot (1999). Fig. 9 shows a comparison for the radiation prediction from the CR model using both the ViSpeN chemisty model and the multi-temperature averaged NASA Ames rate close to the rate of Park (1993) since we are close to a thermal equilibrium state ($T = T_v$). It can be seen that by including a vibrationally specific model, it greatly improves the agreement in terms of the initial rise, absolute intensity level and fall-off rates. This is due to each vibrational state of nitrogen having its individual reaction rate, as opposed to an averaged rate for all states and that the higher level vibration states require less energy to dissociate. Due to the flow being highly nonequilibrium, it is expected that distribution of N_2 vibrational states will also be in non-equilibrium. The amount of molecular nitrogen is most important for the above-equilibrium production of CN through the reaction $C + N_2 \leftrightarrow CN + N$. Immediately behind the shock, there is above equilibrium concentrations of N_2 and C forming quickly through the decay of CH_4. Initially, there are very few N atoms and this is what

allows the reaction to continue beyond equilibrium. The N atoms play an important role in reducing the CN concentration after it has reached the above equilibrium levels. The reverse reaction is responsible for the rapid decay of the CN population. Due to the production of N being faster in the ViSpeN model the reverse reaction occurs faster, reducing the levels of CN quicker. This is consistent with the fall-off rate of the radiation being quicker in the ViSpeN model when compared to the previous CR model. The next step is to include the vibrationally specific rates derived from the NASA Ames database.

6. Further development

In this work, we have used the NASA Ames database for rovibrational rates to derive multi-temperature dissociation rates. We have developed a 0-D state-to-state vibrational collisional model for a detailed study of the dissociation process dynamics and its coupling with the vibrational energy relaxation. Different aspects could be examined in the future:

- A complete rovibrational state-to-state collisional model could be developed to study the dynamics of the internal energy relaxation and dissociation process without any *a priori* assumption on the internal energy distribution. In particular, a comparison with the vibrational state-to-state collisional model would allow the study of deviations of the rotational energy level population from a Boltzmann distribution, this assumption being used often in standard models.
- The complete rovibrational state-to-state collisional model could also be used as a reference model to develop a reduced model based on a different method to sort energy levels. For example, one could lump rovibrational levels as a function of their energy, independently of a separate contribution of their vibrational and rotational energies. This approach is under study and will be described in a separate paper.
- We have shown here that the study of the dynamics of the relaxation and dissociation phenomena could provide some interesting "macroscopic" information on the vibrational energy relaxation times and global dissociation rates. We plan to study different typical conditions by means of the 0-D state-to-state vibrational collisional model to derive a new set of relevant values of vibrational energy relaxation times and global dissociation rates.

Acknowledgments

The authors would like to thank Prof. P. Moin and Prof. G. Iaccarino for their hospitality. The authors have benefitted from helpful discussions with Prof. R. MacCormak and Dr. S. Moreau at Stanford, Dr. A. Bultel and Prof. C. Laux in France, and Prof. O. Chazot in Belgium.

REFERENCES

Bose, D., Wright, M. J., Bogdanoff, D. W., Raiche, G. A. **and** Allen, G. A. 2005 Modeling and experimental validation of CN radiation behind a strong shock wave. *AIAA-2005-768, 43rd AIAA Aerospace Sciences Meeting and Exhibition*, Reno, NV, Jan. 10-13.

Brandis, A. M., Morgan, R. G., McIntyre T., **and** Jacobs, P. A. 2008 Non-equilibrium radiation intensity measurements in simulated Titan atmospheres. *AIAA-2008-4136, 26th AIAA Aerodynamic Measurement Technology and Ground Testing Conference*, Seattle, WA, June 23-26.

Bultel, A., Cheron, B., Bourdon, A., Motapon, O. and Schneider, I. 2006 Collisional-radiative model in air for earth re-entry problems. *Physics of Plasmas* **13**(4) 11.

Chernyi, G. G., Losev, S. A., Macheret, S. O. and Potapkin, B. V. 2004 Physical and chemical processes in gas dynamics: physical and chemical kinetics and thermodynamics of gases and plasmas. *Progress in Astronautics and Aeronautics Series, V-197, AIAA*, Reston, VA.

Esposito, F., Armenise, I. and Capitelli, M. 2006 N-N_2 state to state vibrational-relaxation and dissociation rates based on quasiclassical calculations. *Chemical Physics*, **331**(1) 1.

Gökcen T. 2004 N_2-CH_4-Ar chemical kinetic model for simulations of atmospheric entry to Titan. *AIAA 2004-2469, 37th AIAA Thermophysics Conference*, Portland, OR, June 28-July 1.

Jaffe, R., Schwenke, D., Chaban G. and Huo., W. 2008 Vibrational and rotational excitation and relaxation of nitrogen from accurate theoretical calculations. *AIAA 2008-1208, 46th AIAA Aerospace Sciences Meeting and Exhibit*, Reno, NV, Jan 7-10.

Laux., C.O. 2002 Radiation and non-equilibrium collisional radiative models. *VKI-LS 2002-07, Physico-chemical models for high enthalpy and plasma flows*, Rhode-Saint-Genèse, Belgium.

Macheret, S. O. and Adamovich, I. V. 2000 N-N_2 semiclassical Modeling of State-Specific Dissociation Rates in Diatomic Gases. *Chemical Physics*, **113**(17) 7351.

Magin, T. E., Caillault, L., Bourdon, A. and Laux, C. O. 2006 Non-equilibrium radiative heat flux modeling for the huygens entry probe. *Journal of Geophysical Research - Planets*, **111** E07S12.

Park, C. 1990 *Nonequilibrium hypersonic aerothermodynamics*. Wiley, New York, NY.

Park, C. 1993 Review of chemical-kinetic problems of future NASA mission, I: Earth entries. *Journal of Thermophysics and Heat Transfer*, **7**(3) 385.

Park, C. 2006 Thermochemical relaxation in shock-tubes. *Journal of Thermophysics and Heat Transfer*, **20**(4) 689.

Pierrot, L. 1999 Chemical kinetics and vibrationally-specific collisional-radiative models for non-equilibrium nitrogen plasmas. *Final Report of ESA Post-doctoral Fellowship.* Stanford University, Stanford, CA.

Schwenke, D. 1990 A theoretical prediction of hydrogen molecule dissociation-recombination rates including an accurate treatment of internal state non-equilibrium effects. *J. Chem. Phys.*, **92** 7267.

Schwenke, D., Chaban, G., Jaffe, R. and Huo, W. 2008 Dissociation cross-sections and rate coefficients for nitrogen from accurate theoretical calculations. *AIAA 2008-1209, 46th AIAA Aerospace Sciences Meeting and Exhibit*, Reno, NV, Jan 7-10.

Shatalov, O. P. 1987 Recommended data on rate constants of physical and chemical processes in N-O atoms system. *Tech. Rept.*, Moscow State Univ., Inst. of Mechanics Avogadro Center, Russia.